polymer papers

X-ray and neutron scattering studies of poly(ester carbonate)/poly(ethylene terephthalate) alloys

N. S. Murthy and S. M. Aharoni
Corporate Technology, Allied Corporation, Morristown, New Jersey 07960, USA
(Received 8 September 1986; revised 10 April 1987; accepted 3 June 1987)

Quenched blends of poly(ester carbonate) (PEC) and poly(ethylene terephthalate) (PET) have a single T_g and behave as single-phase amorphous alloys up to 67% PET. However, small-angle neutron scattering (SANS) data show that the PET molecules are not statistically distributed as classical Gaussian coils in the PEC matrix. In quenched amorphous PEC-rich films (a single phase), PET-rich domains of varying PET concentration appear to be randomly distributed in the PEC matrix, and the excess SANS intensity is attributable to fluctuations in PET concentrations. Wide- and small-angle X-ray scattering data and SANS results show incomplete phase separation of PET and PEC molecules upon annealing. A possible model for annealed blends (two phases) might be domains of folded-chain, crystalline PET with interlamellar amorphous regions composed of a mixture of PET and PEC molecules. These domains are dispersed in the amorphous PEC matrix.

(Keywords: PEC/PET alloys; X-ray and SANS studies)

INTRODUCTION

In a recent report[1] the thermal, rheological and mechanical behaviour, crystallization kinetics, morphology and structure of aromatic poly(ester carbonate)/poly(ethylene terephthalate) alloys (PEC/PET) were described. From these studies it became apparent that: (1) the melt viscosity of PEC/PET alloys drops drastically (from 16000 to 4000 Pa) with the addition of small amounts (~2%) of PET; and (2) the blend has a single, rather sharp, composition-dependent T_g for all clear glassy compositions (up to 67% PET). The purpose of the X-ray and neutron scattering experiments described here was to understand how this behaviour is related to the distribution of PET molecules in the PEC matrix, and to follow the segregation of PET as the blend is annealed.

EXPERIMENTAL

Materials

Fully deuterated PET was synthesized in our laboratories ($M_w/M_n \leqslant 2$). A physical mixture of PEC and deuterated PET (both with an intrinsic viscosity of 0.53 dl g^{-1}; M_w(PEC) ~ 21 800, M_w(PET) ~ 40 500) were mixed in the ratio of 98:2 and 90:10. The mixture was dissolved in trichloroethane/phenol solvent. The polymer mixture was precipitated with a large excess of methanol and dried at 80°C overnight under 1 mm vacuum. The resulting fine powder was moulded into thin films at temperatures between 270 and 285°C, and quick-quenched in ice–water to ensure that the sample was amorphous. The films were annealed at 200°C for durations ranging from 5 to 150 min. Ester interchange reactions in PET are known to occur rapidly in the melt and at a much slower rate for temperatures 15°C below T_m (225°C)[2]. In our experiments, such transesterification of the polymer chains in the melt were inhibited by eliminating all polymerization catalysts in PET-d. Selective dissolution of PEC from such films in ethylene dichloride have shown no ester groups (deuterated residue) in the soluble portion, and the insolubles contained no carbonate residues.

Methods

Wide-angle X-ray diffraction (WAXD) patterns were obtained in the parafocus mode on a Philips diffractometer with Cu Kα radiation (graphite monochromator in the diffracted beam). Small-angle X-ray scattering (SAXS) data were obtained on a Franks' camera using Ni-filtered Cu radiation and a position-sensitive proportional counter. Some SAXS data were also obtained using the 10 m SAXS instrument at the National Center for Small Angle Scattering Research (NCSASR) at Oak Ridge National Laboratory. Neutron scattering data (SANS) were obtained on the NCSASR 30 m instrument[3]. Neutrons of 4.75 Å wavelength ($\Delta\lambda/\lambda \simeq 5 \times 10^{-2}$) were collimated with pinholes and counted with a position-sensitive area detector. Two-dimensional scattering data were corrected for background intensity, sample-cell scattering and sample thickness and transmission. The isotropic two-dimensional scattering data were radially averaged to one-dimensional form and reduced to units of absolute differential scattering cross section per unit solid angle, $d\Sigma(Q)/d\Omega$, (cm^{-1}, ±5%) by calibration of the instrument with an irradiated aluminium secondary standard[4]. This standard was in turn calibrated by use of the incoherent scattering from water and vanadium and the coherent scattering from a well characterized, partially labelled polystyrene sample. The overall range of Q studied was $0.0032 < Q = 4\pi\lambda^{-1} \sin\theta < 0.035$ Å^{-1} where 2θ is the angle of scatter. One sample (98:2 PEC:PET-d, 150 min anneal) was run on the NCSASR double-crystal instrument[3], which is capable of much higher resolution ($0.00071 < Q < 0.0059$ Å^{-1}).

0032-3861/87/0032-3861/87/132171-05$03.00

Analysis

The WAXD, SAXS and SANS data will be used to understand the distribution of PET molecules or segments in the amorphous PEC matrix, to study the changes in this distribution upon annealing and to follow the crystallization of PET in PEC/PET blends.

In a WAXD pattern, the PEC contribution consists of two amorphous halos at $2\theta = 18°$ and 27°. Superimposed on this is the amorphous halo of PET at $2\theta = 23°$. Thus, it is difficult to determine the crystallinity of PET alone. However, one can determine the ratio of the area under the crystalline peaks to the area under the entire scattering curve. Since PEC does not crystallize, this ratio will be used as a relative measure of PET crystallinity within this series of experiments.

The lamellar spacing of PET crystallites was calculated by applying Bragg's law to the position of the peak maximum in the small-angle X-ray scattering curve. The area under the small-angle peak was determined after drawing a background by extending the scattering curves from either side of the peak.

The small-angle neutron scattering curves were analysed by using the programs available at the NCSASR. The scattering curves from PET-h(10%)/PEC(90%) and 100% PEC were mostly h-incoherent with angle-independent cross sections of 1.0 and 0.7 cm^{-1} respectively. Incoherent backgrounds were subtracted from PEC/PET-d data. Since PET-d samples were prepared by methods identical to that of PET-h, using the same catalysts and same procedures, and because the scattering from PET-h(10%)/PEC(90%) and 100% PEC is angle-independent, we assumed that the impurities in PET-d do not give rise to angle-dependent scattering, especially at low angles. Scattering in samples containing PET-d therefore is attributed to structural features. The low-angle region was analysed by using Zimm ($1/I$ vs. Q^2) and Guinier ($\ln I$ vs. Q^2) plots[5,6]. The high-angle data were analysed using Porod (IQ^4 vs. Q) and Soulé–Porod (IQ^4 vs. Q^4) plots. The lower-Q data were used to analyse the size and distribution of PET-rich domains. In these partially segregated systems, we neglected interparticle (i.e. interdomain) interference, and we calculated the domain sizes by Guinier analysis. The higher-angle data were used to analyse the electron-density fluctuations within the domains.

RESULTS AND DISCUSSION

Figure 1 shows wide-angle X-ray diffraction (WAXD) scans of PEC (*Figure 1a*), PET (*Figure 1b*), and 90:10 PEC/PET-d before annealing, i.e. quick-quenched (*Figure 1c*), and after annealing at 200°C for 150 min (*Figure 1d*). No crystalline features are visible in the quenched film, and the crystalline peaks in the annealed film are due to PET. The area under the crystalline peaks (*Figure 1d*), a relative measure of the fraction of the

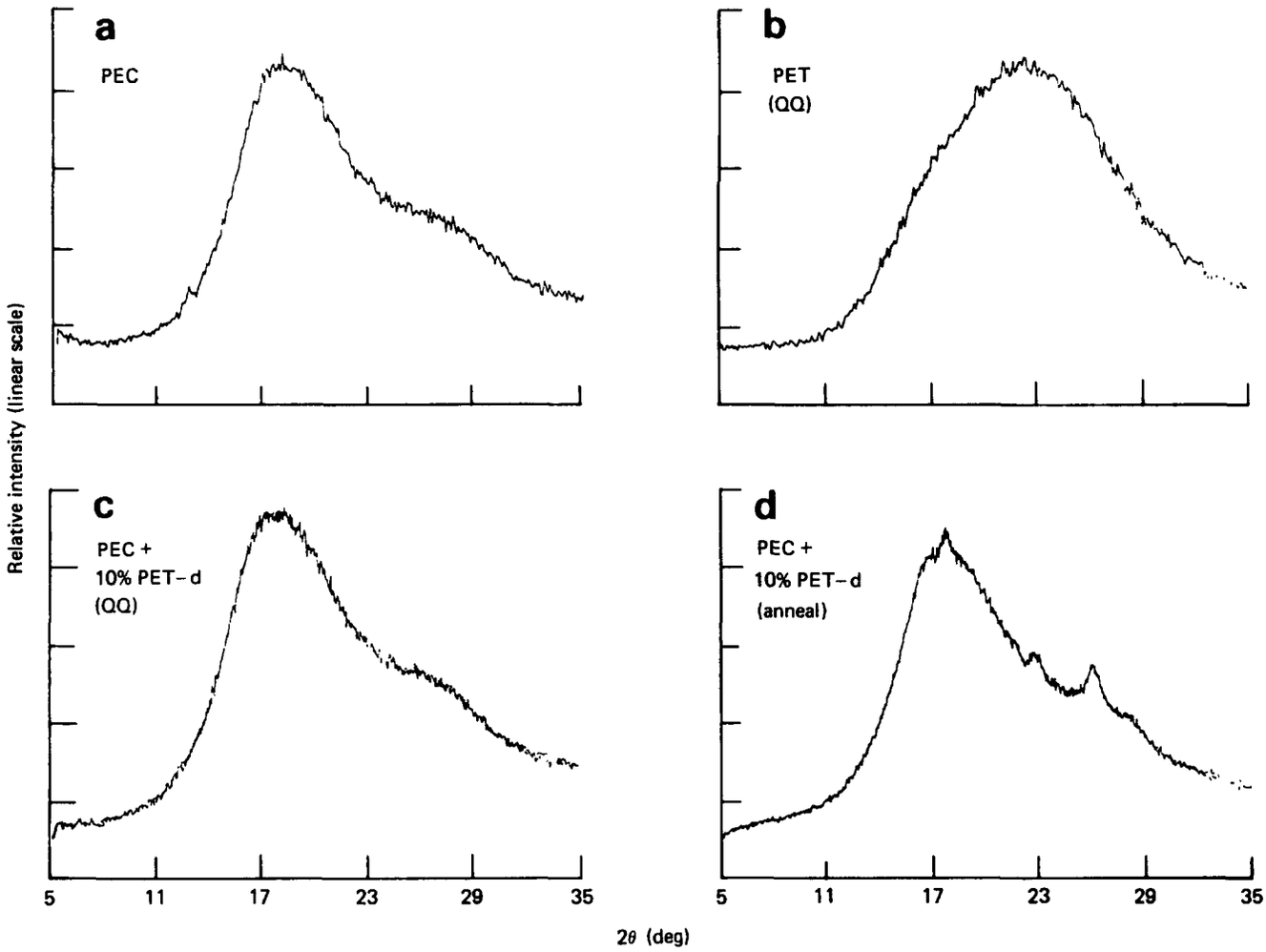

Figure 1 Wide-angle X-ray diffraction scans: (a) poly(ester carbonate), PEC; (b) quenched poly(ethylene terephthalate), PET; (c) quenched alloy of PEC/PET-d (90:10); (d) annealed (200°C, 150 min) alloy of PEC (90%) and PET-d (10%)

crystallized PET, is plotted in *Figure 2* as a function of duration of annealing. The features of such curves have been discussed earlier[1]. In summary, the crystallization kinetics of PET in the blend is characterized by a period of slow growth (induction time ~ 10 min) followed by a period of rapid primary crystallization ($t_{1/2} \sim 1$ h). Beyond this point (not shown in *Figure 2*), slow secondary crystal growth occurs. Both the induction time and $t_{1/2}$ for the primary crystallization are longer than for pure PET (10 s and 40 s respectively). Thus, although a substantial fraction of PET crystallizes out of the PET/PEC matrix, it crystallizes at a far slower rate than in pure PET.

Figure 3 shows SAXS curves of 90:10 alloy before and after annealing for 5, 30, 60 and 150 min. The large intensity near zero angle in these SAXS curves is probably due to electron-density fluctuations arising from structures or long-range correlations which might be present even in quenched films. As will be shown later, these same fluctuations also give rise to large SANS intensity at zero angles. The Bragg spacing corresponding

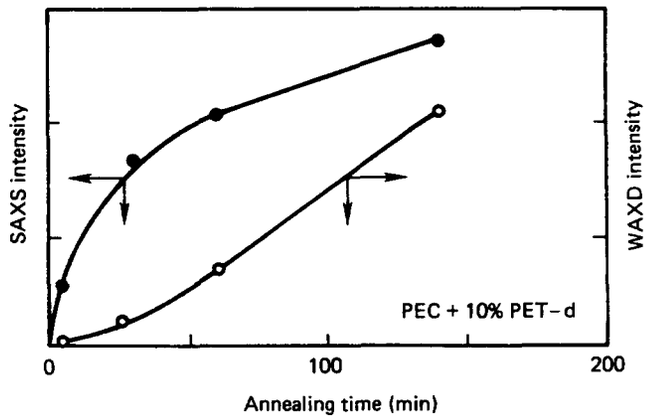

Figure 2 Changes in SAXS lamellar intensity and WAXD crystalline intensity as a function of annealing time

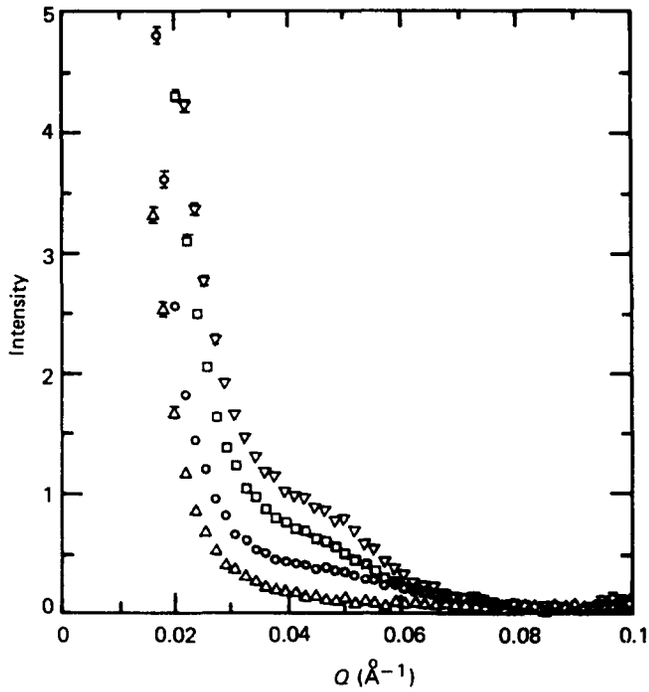

Figure 3 SAXS curves of 90:10 PEC/PET-d at annealing times of 0 min (△), 30 min (○), 60 min (□) and 150 min (▽)

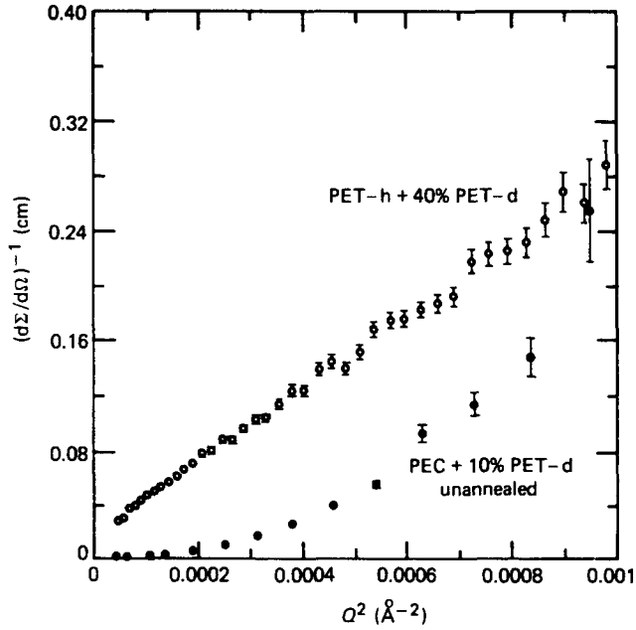

Figure 4 Zimm plots of labelled PET-d in PET, and in PEC (10% PET-d, unannealed)

to the peak maximum is ~135 Å and does not change with annealing time. The intensity of the small-angle peak, however, does increase with the length of annealing (*Figure 2*), and, unlike what is suggested by the WAXD data, there appears to be no induction time. The increase in SAXS intensity suggests an increase in crystalline order (increase in contrast), and the growth (increase in the number or size) of the lamellae or PET-rich domains. A comparison of SAXS and WAXD intensity suggests that large-scale PET-rich structures are first formed and become detectable, before one can observe any local crystalline order. It is thus possible that PET molecules first segregate into PET-rich domains, form lamellae and then, after an induction time of 10 min, crystallize within these domains.

Although PET is amorphous in quenched films (*Figure 1c*), it does not exist as a separate phase since only one T_g is observed. SANS were analysed to study the distribution of PET in these single-phase quenched films. Lower-angle SANS were analysed using Zimm and Guinier plots. If the PET molecules were molecularly dispersed as Gaussian coils, then one would expect to see a linear Zimm plot with a zero-Q cross section, $d\Sigma(0)/d\Omega$, characteristic of a single chain, as shown in *Figure 4* (open circles) from a sample where the PET-d molecules are molecularly dispersed in a PET-h matrix[7]. The Zimm plots for all PET/PEC blends (typical results are shown in *Figure 4* (full circles)) were not linear, indicating that the PET-d molecules are not molecularly dispersed as individual coils in the PEC matrix even in quenched films. The SANS intensity therefore arises from the fluctuations in the concentration of the PET molecules in the PEC matrix.

If we assume a two-phase system for annealed samples, i.e. a model in which the PET-d molecules are completely phase-separated in a matrix of PEC-h, we expect to see a linear Guinier plot whose slope is characteristic of the domain dimensions, going over to Q^{-4} behaviour at higher Q in the Porod region, if the boundaries between the two phases are sharp. Although one could fit a straight line to the first few points in a Guinier plot

(*Figure 5*), the fit does not extend over a wider range. The data from the double-crystal instrument ($Q_{min} = 0.007$ Å^{-1}) on 98:2 PEC/PET-d (150 min anneal) continued to show a positive curvature (positive deviation from Guinier law), indicating that the scattering particles are highly polydisperse. The values obtained from such plots of the data from the 30 m instrument ($0.0032 < Q < 0.0055$ Å^{-1}, *Table 1*) therefore represent a lower limit. Secondly, the Porod constant, instead of being equal to 4.0, varies from 3.55 to 4.45 (*Table 1*), indicating deviations from an ideal two-phase system with a sharp boundary between the phases. Thirdly, a comparison of the calculated and measured values of the zero-Q cross section, $d\Sigma(0)/d\Omega$, shows that the theoretical value calculated from the Guinier model assuming a two-phase system is four times the experimental value. The measured and theoretical values from the double-crystal instrument data are 62×10^3 and 489×10^3 cm^{-1} (ratio of theory to experiment = 8) respectively. These results suggest that we have an intermixed or interdispersed multiphase system and that the phase separation is not complete even in the annealed samples.

To understand better the incomplete phase separation of the PET and PEC molecules, we considered the wide- and small-angle X-ray scattering results together with the SANS data in *Table 1*. The domain size, $r = (5R_g^2/3)^{1/2}$, estimated from the Guinier plot ($0.0032 < Q < 0.0055$ Å^{-1}) is ~700 Å. This is a lower limit for r because of the angular range and interparticle interference. The value for 98:2 PEC/PET (150 min anneal) from data in the range of even lower Q (~0.0007 Å^{-1}) is 1600 Å. It is possible that PET-rich domains of PEC, ~1000 Å in radius, are randomly distributed in the pure PEC matrix. In the quenched materials, PET might exist as small amorphous aggregates in PET-rich domains. In annealed samples, results of the Guinier analysis of the SANS data assuming a two-phase system (*Table 1*) show that PET molecules are not completely phase-separated. On the other hand, SAXS data show a repeat of 135 Å typical of PET lamellae (*Figure 3*) and WAXD shows the existence of crystalline PET with a coherence length of ~100 Å (*Figure 1d*). These suggest that within a scattering particle of ~1000 Å radius, we might have lamellar PET crystallites, with a mixture of PET and PEC in the interlamellar regions. These PET-rich domains are uniformly distributed in the PEC matrix. This model accounts for the polydispersity of the scattering particle (non-linear Guinier curve in *Figure 5*). Large inhomogeneities, due to crystallized PET within the scattering domain, are confirmed by the positive

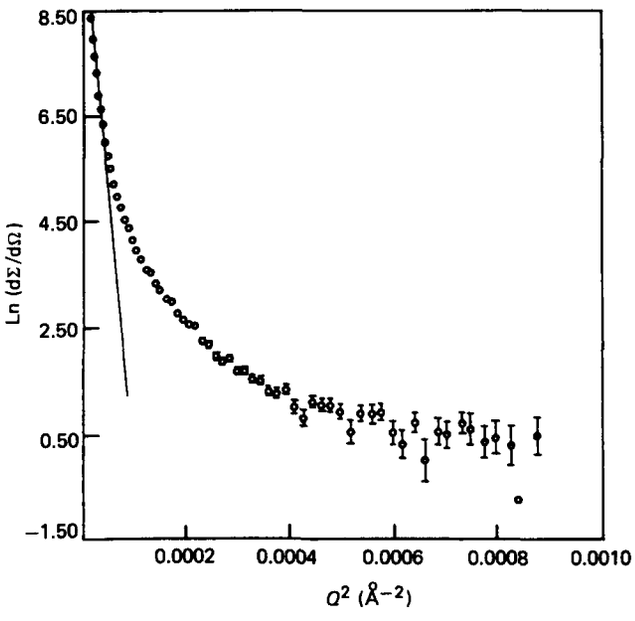

Figure 5 Guinier plot of the 98:2 PET-d/PEC sample annealed at 200°C for 150 min

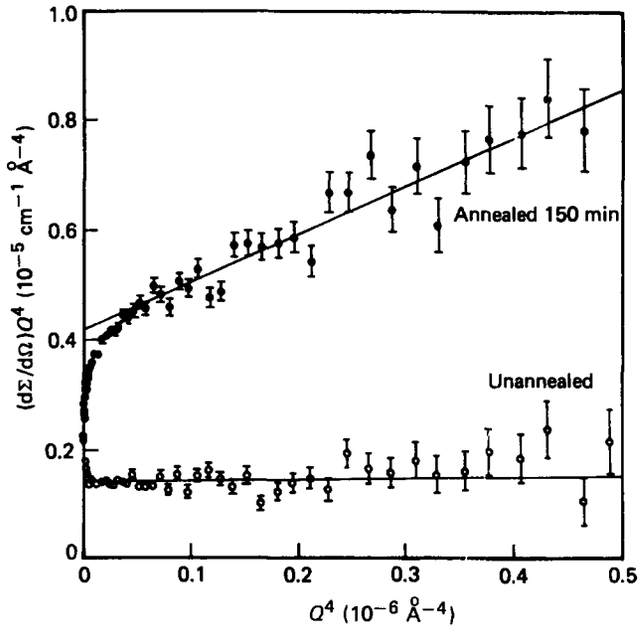

Figure 6 Soulé–Porod plots for 90:10 alloy of PEC/PET-d from quick-quenched (unannealed) and annealed (150 min at 200°C) films

Table 1 Parameters derived from SANS data

Sample	Annealing time (min)	Particle size, $r=(5R_g^2/3)^{1/2}$	Porod power, N	Guinier model, $d\Sigma(0)/d\Omega$ (cm^{-1})			Porod constant (cm^{-1} Å^{-4})			Porod slope, IQ^4 vs. Q^4
				Exp.	Theory	Theory / Exp.	Exp.	Theory	Theory / Exp.	
98:2	0	696								
	10	687	4.1	8.7×10^3	37×10^3	4.3	0.44×10^{-6}	0.73×10^{-6}	1.7	*
	150	684	4.2	11.6	37	3.2	0.54	0.63	1.2	*
90:10	0	803								
	30	751	4.2	65	243	3.8	2.0	4.31	2.2	5.1
	60	772	3.9	63	269	4.2	3.23	4.20	1.3	7.5
	150	661	3.6	43	166	3.9	4.17	4.90	1.2	8.8

* Data too noisy for the evaluation of the slope

deviations from Porod's law (*Figure 6*)[8]. Any futher refinement of this model consisting of PET crystallites, mixture of amorphous PET and PEC, and amorphous PEC requires more elaborate experiments and data analyses. Our preliminary results show that the tremendous drop in melt viscosity and single T_g are not due to molecularly dispersed PET, but due to intermixing of amorphous PET and PEC, representing a partially compatible (miscible in the amorphous phase) system.

ACKNOWLEDGEMENTS

We are deeply indebted to Dr G. D. Wignall for his help in carrying out SANS experiments, in interpreting the results and for his valuable comments during the preparation of this manuscript. We also thank Dr D. K. Christen for kindly providing the data from the double-crystal instrument for one of the samples. This research was sponsored by Allied Corporation and the National Science Foundation under Grant DMR-77 24459, with the US Department of Energy under Contract DE-AC05-840R21400 with Martin Marietta Energy Systems Inc.

REFERENCES

1 Aharoni, S. M. *J. Macromol. Sci.–Phys.* 1983–84, **B22**, 813
2 McAlea, K. P., Schultz, J. M., Gardner, K. H. and Wignall, G. D. *Polymer* 1986, **27**, 1581
3 Koehler, W. C., Hendricks, R. W., Child, J. R., King, S. P., Lin, J. S. and Wignall, G. D. 'Scattering Techniques Applied to Supramolecular and Nonequilibrium Systems', (Eds. S. Chen, B. Chu and R. Nossal), Plenum Press, New York, NATO Advanced Study Series, Vol. 83, 1981, p. 75
4 Zimm, B. H. *J. Chem. Phys.* 1948, **16**, 157
5 Wignall, G. D. and Bates, F. S. *J. Appl. Crystallogr.* 1987, **20**, 28
6 Guinier, A. and Fournet, G. 'Small-Angle Scattering of X-Rays', Wiley, New York, 1955
7 McAlea, K. P., Schultz, J. M., Gardner, K. H. and Wignall, G. D. *Macromolecules* 1985, **18**, 447
8 Ruland, W. *J. Appl. Crystallogr.* 1971, **4**, 70